

Soft gluon corrections to double transverse-spin asymmetries for small- Q_T dilepton production at RHIC and J-PARC

HIROYUKI KAWAMURA^a, JIRO KODAIRA^{b*} AND KAZUHIRO TANAKA^c

^a *Radiation Laboratory, RIKEN, Wako 351-0198, Japan*

^b *Theory Division, KEK, Tsukuba 305-0801, Japan*

^c *Department of Physics, Juntendo University, Inba, Chiba 270-1695, Japan*

Abstract

We calculate the double transverse-spin asymmetries, $\mathcal{A}_{TT}(Q_T)$, in transversely polarized Drell-Yan process at the transverse-momentum Q_T of the produced lepton pair. We perform all-order resummation of the logarithmically enhanced contributions in the relevant Drell-Yan cross sections at small Q_T , which are due to multiple soft gluon emission in QCD, up to the next-to-leading logarithmic accuracy. The asymmetries $\mathcal{A}_{TT}(Q_T)$ to be observed in polarized experiments at RHIC and J-PARC are studied numerically as a function of Q_T . We show that the effects of the soft gluon resummation to the polarized and unpolarized cross sections largely cancel in $\mathcal{A}_{TT}(Q_T)$, but the significant corrections still remain and are crucial for making a reliable QCD prediction of $\mathcal{A}_{TT}(Q_T)$. In particular, the soft gluon corrections enhance $\mathcal{A}_{TT}(Q_T)$ considerably in the small Q_T region compared with the asymmetry in the fixed-order α_s perturbation theory. We also derive a novel asymptotic formula which embodies those remarkable features of $\mathcal{A}_{TT}(Q_T)$ at small Q_T in a compact analytic form and is useful to extract the transversity $\delta q(x)$ from the experimental data.

*Deceased.

1 Introduction

In recent years, a variety of experiments has been devoted to explore the spin-dependent phenomena in hard processes. Especially, experiments with transversely polarized hadrons have opened a new window to study rich structure of perturbative/nonperturbative dynamics of QCD associated with the transverse spin [1]. One of the fundamental quantities which newly enter into play is the chiral-odd, twist-2 parton distribution, called the transversity $\delta q(x)$; it represents the distribution of transversely polarized quark inside transversely polarized nucleon, i.e, the partonic structure of the nucleon which is complementary to that associated with the other twist-2 distributions, such as the familiar density and helicity distributions $q(x)$ and $\Delta q(x)$. However, $\delta q(x)$ has not been well-known so far. This is because $\delta q(x)$ cannot be measured in inclusive DIS in contrast to $q(x)$ and $\Delta q(x)$; the chiral-odd nature requires a chirality flip, so that $\delta q(x)$ must be always accompanied with another chiral-odd function in physical observables. It is very recent that the first global fit of $\delta q(x)$ is given [2] using the semi-inclusive DIS data, in combination with the e^+e^- data for the associated chiral-odd (Collins) fragmentation function.

Transversely polarized Drell-Yan (tDY) process, $p^\uparrow p^\uparrow \rightarrow l^+ l^- X$, is another promising process to access the transversity $\delta q(x)$. Based on QCD factorization, the spin-dependent cross section $\Delta_T d\sigma \equiv (d\sigma^{\uparrow\uparrow} - d\sigma^{\uparrow\downarrow})/2$ is given as a convolution, $\Delta_T d\sigma = \int dx_1 dx_2 \delta H(x_1, x_2; \mu_F^2) \Delta_T d\hat{\sigma}(x_1^0/x_1, x_2^0/x_2; Q^2, \mu_F^2/Q^2)$, where Q is the dilepton mass, μ_F is the factorization scale,

$$\delta H(x_1, x_2; \mu_F^2) = \sum_q e_q^2 [\delta q(x_1, \mu_F^2) \delta \bar{q}(x_2, \mu_F^2) + \delta \bar{q}(x_1, \mu_F^2) \delta q(x_2, \mu_F^2)], \quad (1)$$

is the product of transversity distributions of the two nucleons, summed over the massless quark flavors q with their charge squared e_q^2 , and $\Delta_T d\hat{\sigma} = (d\hat{\sigma}^{\uparrow\uparrow} - d\hat{\sigma}^{\uparrow\downarrow})/2$ is the corresponding partonic cross section. $x_1^0 = \sqrt{\tau} e^y, x_2^0 = \sqrt{\tau} e^{-y}$ are the relevant scaling variables, where $\tau = Q^2/S$, and \sqrt{S} and y are the total energy and dilepton's rapidity in the nucleon-nucleon CM system. At the leading twist level, the gluon does not contribute to the transversely polarized, chiral-odd process, corresponding to helicity-flip by one unit. The unpolarized cross section, $d\sigma \equiv (d\sigma^{\uparrow\uparrow} + d\sigma^{\uparrow\downarrow})/2$, obeys factorization similar as $\Delta_T d\sigma$, in terms of $H(x_1, x_2; \mu_F^2)$ that is given by (1) with $\delta q \rightarrow q$ and $\delta \bar{q} \rightarrow \bar{q}$, and additional functions involving the gluon distribution that comes in as higher-order α_s corrections. Therefore, the double-spin asymmetry in tDY, $A_{TT} \equiv \Delta_T d\sigma/d\sigma$, in principle provides clean information on the transversity $\delta q(x)$. At the leading order (LO) in QCD perturbation theory, $x_{1,2}^0$ coincide with the momentum fractions carried by the incident partons, e.g., $\Delta_T d\hat{\sigma} \propto \delta(x_1 - x_1^0) \delta(x_2 - x_2^0)$, so that [3, 1]

$$A_{TT} = \frac{\Delta_T d\sigma}{d\sigma} = \frac{1}{2} \cos(2\phi) \frac{\delta H(x_1^0, x_2^0; Q^2) + \dots}{H(x_1^0, x_2^0; Q^2) + \dots}, \quad (2)$$

where ϕ denotes the azimuthal angle of one of the leptons with respect to the incoming nucleon's spin axis, and the ellipses stand for the QCD corrections of NLO or higher. The $\cos(2\phi)$ dependence is characteristic of the spin-dependent cross section $\Delta_T d\sigma$ of tDY [3].

A_{TT} to be observed in tDY at RHIC-Spin experiment was calculated by Martin et al. [4] including the NLO QCD corrections. The results are somewhat discouraging in that the corresponding A_{TT} are at most a few percent [4]. * The reason is twofold (see (2)): (i) tDY in pp collisions probes the product of the quark transversity-distribution and the antiquark one as (1), and the latter is likely to be small; (ii) the rapid growth of the unpolarized sea-quark distributions in $H(x_1^0, x_2^0; Q^2)$ is caused by the DGLAP evolution in the low- x region that is typically probed at RHIC, $\sqrt{S} = 200$ GeV, $Q \lesssim 10$ GeV, and $\sqrt{\tau} \lesssim 0.05$. Thus, small A_{TT} at RHIC appears to be rather general conclusion (see also [5]).

We note that those previous NLO studies of A_{TT} of (2) correspond to tDY with the transverse-momentum Q_T of the produced lepton pair unobserved, and use the cross sections $\Delta_T d\sigma, d\sigma$ integrated over Q_T in (2). However, in view of the fact that most of the lepton pairs are actually produced at small Q_T in experiment, it is important to examine the double transverse-spin asymmetries at a measured Q_T , in particular its behavior for small Q_T . This is defined similarly as (2) using the “ Q_T -differential” cross sections, and we denote it as $\mathcal{A}_{TT}(Q_T)$ distinguishing from the conventional Q_T -independent A_{TT} . In fact, participation of the new scale $Q_T (\ll Q)$ causes profound modifications of the relevant theoretical framework. For example, now the numerator and the denominator of $\mathcal{A}_{TT}(Q_T)$ may involve the parton distributions associated with the scales $\sim Q_T$, such as $\delta H(x_1^0, x_2^0; Q_T^2)$ and $H(x_1^0, x_2^0; Q_T^2)$, respectively. For $H(x_1^0, x_2^0; Q_T^2)$, the low- x rise of the unpolarized sea-quark distributions, mentioned in (ii) above, is milder compared with $H(x_1^0, x_2^0; Q^2)$. Thus, if the former components play dominant roles compared with the latter in the denominator of $\mathcal{A}_{TT}(Q_T)$ by certain partonic mechanism, $\mathcal{A}_{TT}(Q_T)$ for small Q_T region at RHIC can be larger than A_{TT} ; the necessary partonic mechanism is indeed provided as the large logarithmic contributions of the type $\ln(Q^2/Q_T^2)$, which is another remarkable consequence of the new scale Q_T : the small transverse-momentum Q_T of the final lepton pair is provided by the recoil from the emission of soft gluons which produces the large terms behaving as $\alpha_s^n \ln^m(Q^2/Q_T^2)/Q_T^2$ ($m = 0, 1, \dots, 2n - 1$) at each order of perturbation theory for the tDY cross sections. Actually, such enhanced “recoil logarithms” spoil the fixed-order perturbation theory, and have to be resummed to all orders in α_s to make a reliable prediction of the cross sections at small Q_T . Recently, we have worked out the corresponding “ Q_T -resummation” for the tDY cross sections up to next-to-leading logarithmic (NLL) accuracy, which corresponds to summing up exactly the first three towers of logarithms, $\alpha_s^n \ln^m(Q^2/Q_T^2)/Q_T^2$ with $m = 2n - 1, 2n - 2$ and $2n - 3$, for all n [6]. Utilizing this result, in the present paper, we develop QCD prediction for $\mathcal{A}_{TT}(Q_T)$ as a function of Q_T .

We will demonstrate that the soft gluon corrections are significant so that $\mathcal{A}_{TT}(Q_T)$ in the small Q_T region is considerably large compared with the known value for A_{TT} . † In addition to $\mathcal{A}_{TT}(Q_T)$ in tDY at RHIC, we calculate $\mathcal{A}_{TT}(Q_T)$ to be observed at J-PARC when the polarized beam is realized [7]. The latter case is also interesting because the fixed target experiments at J-PARC probe the parton distributions in the medium x region

*In [4], the corresponding asymmetries are defined through certain integration over ϕ , and equal (2) with the formal replacement $\cos(2\phi) \rightarrow 2/\pi$.

†For the impact of the Q_T resummation on the spin asymmetries in semi-inclusive deep inelastic scattering, see [8].

($\sqrt{S} = 10$ GeV, $Q \gtrsim 2$ GeV, and $\sqrt{\tau} \gtrsim 0.2$), and thus large asymmetries are expected even for the Q_T -independent A_{TT} [9] (see (ii) above). We also find that $\mathcal{A}_{TT}(Q_T)$ for $Q_T \approx 0$ deserves special attention from theoretical as well as experimental point of view, and derive a compact analytic formula for $\mathcal{A}_{TT}(Q_T \approx 0)$.

The paper is organized as follows. In Sec. 2, the Q_T -resummation formula for the tDY cross sections is introduced, and all ingredients necessary for calculating the Q_T -dependent asymmetries $\mathcal{A}_{TT}(Q_T)$ including the NLL resummation contributions are explained. In Sec. 3, numerical results of $\mathcal{A}_{TT}(Q_T)$ at RHIC and J-PARC are presented. Sec. 4 is devoted to the discussion of analytic formula of $\mathcal{A}_{TT}(Q_T)$ at $Q_T \approx 0$ using the saddle-point method. Conclusions are given in Sec. 5.

2 Resummed cross section and asymmetry for tDY

Throughout the paper we employ the $\overline{\text{MS}}$ factorization and renormalization scheme with the corresponding scales, μ_F and μ_R . We first recall basic points of the fixed-order calculation of the spin-dependent, Q_T -differential cross sections of tDY [6]. In the lowest-order approximation via the Drell-Yan mechanism, the lepton pair is produced with vanishing Q_T , so that the corresponding partonic cross section is proportional to $\delta(Q_T^2)$. The one-loop corrections to the partonic cross section involve the virtual gluon corrections, and the real gluon emission contributions, $q + \bar{q} \rightarrow l + \bar{l} + g$; in the latter case, the finite Q_T of the lepton pair is provided by the recoil from the gluon radiation. Those have been calculated in the dimensional regularization [6], and the differential cross section of tDY is obtained as

$$\frac{\Delta_T d\sigma^{\text{FO}}}{dQ^2 dQ_T^2 dy d\phi} = \cos(2\phi) \frac{\alpha^2}{3 N_c S Q^2} [\Delta_T X(Q_T^2, Q^2, y) + \Delta_T Y(Q_T^2, Q^2, y)], \quad (3)$$

where $\Delta_T X$ and $\Delta_T Y$ are, respectively, expressed as the convolution of (1) with the corresponding partonic cross sections, see [6] for their explicit form in the $\overline{\text{MS}}$ scheme: $\Delta_T X = \Delta_T X^{(0)} + \Delta_T X^{(1)}$ as the sum of $\mathcal{O}(\alpha_s^0)$ and $\mathcal{O}(\alpha_s^1)$ contributions, where $\alpha_s = \alpha_s(\mu_R^2)$ with μ_R the renormalization scale, and $\Delta_T X^{(0)} = \delta H(x_1^0, x_2^0; \mu_F^2) \delta(Q_T^2)$. The partonic cross section associated with $\Delta_T X^{(1)}$ contains all terms that are singular as $Q_T \rightarrow 0$, behaving $Q_T^{-2} \times (\ln(Q^2/Q_T^2) \text{ or } 1)$ or $\delta(Q_T^2)$, while the $\mathcal{O}(\alpha_s)$ terms that are less singular than those in $\Delta_T X^{(1)}$ are included in the “finite” part $\Delta_T Y$. In (3), $\Delta_T X$ becomes very large as $\sim \alpha_s \ln(Q^2/Q_T^2)/Q_T^2$ and $\sim \alpha_s/Q_T^2$ when $Q_T \ll Q$, representing the recoil effects from the emission of the soft and/or collinear gluon, and those terms have to be combined with the large contributions of similar nature that appear in each order of perturbation theory as $\alpha_s^n \ln^{2n-1}(Q^2/Q_T^2)/Q_T^2$, $\alpha_s^n \ln^{2n-2}(Q^2/Q_T^2)/Q_T^2$, and so on, from the multiple gluon emission.

The resummation of those logarithmically enhanced contributions to all orders has been worked out [6], in order to obtain a well-defined, finite prediction for the cross section. This is carried out by exponentiating the soft gluon effects in the impact parameter b space, up to the NLL accuracy. As the result, $\Delta_T X$ of (3) is replaced by the corresponding NLL

resummed component as $\Delta_T X \rightarrow \Delta_T X^{\text{NLL}}$, with [6]

$$\Delta_T X^{\text{NLL}}(Q_T^2, Q^2, y) = \sum_{i,j,k} e_i^2 \int_0^\infty db \frac{b}{2} J_0(bQ_T) e^{S(b,Q)} (C_{ij} \otimes f_j) \left(x_1^0, \frac{b_0^2}{b^2} \right) (C_{ik} \otimes f_k) \left(x_2^0, \frac{b_0^2}{b^2} \right). \quad (4)$$

Here $J_0(bQ_T)$ is a Bessel function for the two-dimensional Fourier transformation from the b space to the Q_T space, and $b_0 = 2e^{-\gamma_E}$ with γ_E the Euler constant. The symbol \otimes denotes convolution as $(C_{ij} \otimes f_j)(x, \mu^2) = \int_x^1 (dz/z) C_{ij}(z, \alpha_s(\mu^2)) f_j(x/z, \mu^2)$. Note that the suffix i, j, k can be either q, \bar{q} including the flavor degrees of freedom, and we set $f_q(x, \mu^2) \equiv \delta q(x, \mu^2)$, $f_{\bar{q}}(x, \mu^2) \equiv \delta \bar{q}(x, \mu^2)$. The soft gluon effects are resummed into the Sudakov factor $e^{S(b,Q)}$ with

$$S(b, Q) = - \int_{b_0^2/b^2}^{Q^2} \frac{d\kappa^2}{\kappa^2} \left\{ A_q(\alpha_s(\kappa^2)) \ln \frac{Q^2}{\kappa^2} + B_q(\alpha_s(\kappa^2)) \right\}. \quad (5)$$

The functions A_q , B_q as well as the coefficient functions C_{ij} are perturbatively calculable: $A_q(\alpha_s) = \sum_{n=1}^\infty \left(\frac{\alpha_s}{2\pi}\right)^n A_q^{(n)}$, $B_q(\alpha_s) = \sum_{n=1}^\infty \left(\frac{\alpha_s}{2\pi}\right)^n B_q^{(n)}$, and $C_{ij}(z, \alpha_s) = \delta_{ij} \delta(1-z) + \sum_{n=1}^\infty \left(\frac{\alpha_s}{2\pi}\right)^n C_{ij}^{(n)}(z)$. At the NLL accuracy,

$$A_q^{(1)} = 2C_F, \quad A_q^{(2)} = 2C_F \left\{ \left(\frac{67}{18} - \frac{\pi^2}{6} \right) C_G - \frac{5}{9} N_f \right\}, \quad B_q^{(1)} = -3C_F, \quad (6)$$

where $C_F = (N_c^2 - 1)/(2N_c)$, $C_G = N_c$, and N_f is the number of QCD massless flavors, and

$$C_{ij}^{(1)}(z) = \delta_{ij} C_F \left(\frac{\pi^2}{2} - 4 \right) \delta(1-z) \quad (7)$$

are derived in [6]. The result (6) coincides with that obtained for other processes [10, 11], demonstrating that $\{A_q^{(1)}, A_q^{(2)}, B_q^{(1)}\}$ are universal (process-independent). [‡] Substituting (6) and the running coupling constant $\alpha_s(\kappa^2)$ at two-loop level, the κ^2 integral in (5) can be performed explicitly to the NLL accuracy, and the result can be systematically organized as (see also [13, 14])

$$S(b, Q) = \frac{1}{\alpha_s(\mu_R^2)} h^{(0)}(\lambda) + h^{(1)}(\lambda), \quad (8)$$

where the first and second terms collect the LL and NLL contributions, respectively, as

$$h^{(0)}(\lambda) = \frac{A_q^{(1)}}{2\pi\beta_0^2} [\lambda + \ln(1-\lambda)], \quad (9)$$

$$\begin{aligned} h^{(1)}(\lambda) = & \frac{A_q^{(1)}\beta_1}{2\pi\beta_0^3} \left[\frac{1}{2} \ln^2(1-\lambda) + \frac{\lambda + \ln(1-\lambda)}{1-\lambda} \right] + \frac{B_q^{(1)}}{2\pi\beta_0} \ln(1-\lambda) \\ & - \frac{1}{4\pi^2\beta_0^2} \left[A_q^{(2)} - 2\pi\beta_0 A_q^{(1)} \ln \frac{Q^2}{\mu_R^2} \right] \left[\frac{\lambda}{1-\lambda} + \ln(1-\lambda) \right]. \end{aligned} \quad (10)$$

[‡] $B_q^{(n)}$ ($n \geq 2$) and $C_{ij}^{(n)}(z)$ ($n \geq 1$) depend on the process [12]. Also, $A_q^{(n)}$ ($n = 1, 2, \dots$) and $B_q^{(1)}$ are independent of the factorization scheme, but $B_q^{(n)}$ ($n \geq 2$) and $C_{ij}^{(n)}(z)$ ($n \geq 1$) depend on the factorization scheme (see e.g. [14]).

In these equations, β_0 , β_1 are the first two coefficients of the QCD β function given by $\beta_0 = (11C_G - 2N_f)/(12\pi)$, $\beta_1 = (17C_G^2 - 5C_GN_f - 3C_FN_f)/(24\pi^2)$, and

$$\lambda = \beta_0 \alpha_s(\mu_R^2) \ln \frac{Q^2 b^2}{b_0^2} \equiv \beta_0 \alpha_s(\mu_R^2) L . \quad (11)$$

In the b space, $L = \ln(Q^2 b^2 / b_0^2)$ plays the role of the large logarithmic expansion parameter with $b \sim 1/Q_T$, and λ of (11) is formally considered as being of order unity in the resummed logarithmic expansion to the NLL in (8), where the neglected NNLL corrections are down by $\alpha_s(\mu_R^2)$. Note that, expanding the above NLL formula (4) with (6)-(11) in powers of $\alpha_s(\mu_R^2)$, the first three towers of logarithms, $\alpha_s^n \ln^m(Q^2/Q_T^2)/Q_T^2$ with $m = 2n - 1, 2n - 2$ and $2n - 3$, in the tDY differential cross section are fully reproduced for all n . Combining this expansion with the finite part $\Delta_T Y$ of (3), the result gives the tDY differential cross section which is exact up to $\mathcal{O}(\alpha_s)$; thus we use the NLO parton distributions in the $\overline{\text{MS}}$ scheme for $f_j(x, \mu^2)$ in (4), as well as for those involved in $\Delta_T Y$.

We explain some further manipulations for our NLL formula; those were actually performed in [6], but were not described in detail. The integrand of (4) depends on the parton distributions at the scale b_0/b , according to the general formulation [15]. Taking the Mellin moments of $\Delta_T X^{\text{NLL}}(Q_T^2, Q^2, y)$ with respect to the DY scaling variables $x_{1,2}^0$ at fixed Q ,

$$\Delta_T X_{N_1, N_2}^{\text{NLL}}(Q_T^2, Q^2) \equiv \int_0^1 dx_1^0 (x_1^0)^{N_1-1} \int_0^1 dx_2^0 (x_2^0)^{N_2-1} \Delta_T X^{\text{NLL}}(Q_T^2, Q^2, y), \quad (12)$$

the b -dependence of those parton distributions can be disentangled because the moments, $f_{i,N}(\mu^2) \equiv \int_0^1 dx x^{N-1} f_i(x, \mu^2)$, obey the renormalization group (RG) evolution as $f_{i,N}(b_0^2/b^2) = \sum_j U_{ij,N}(b_0^2/b^2, Q^2) f_{j,N}(Q^2)$, where $U_{ij,N}(\mu^2, \mu'^2)$ are the NLO evolution operators for the transversity distributions which are expressed in terms of the corresponding LO and NLO anomalous dimensions [16, 17] and the two-loop running coupling constant. For (12) with (4) and the above RG evolution substituted, several ‘‘reorganization’’ of the relevant large-logarithmic expansion is necessary for its consistent evaluation over the entire range of Q_T , following the systematic procedure in [14] elaborated for unpolarized hadron collisions: exploiting the RG invariance, we have $C_{ij,N}(\alpha_s(b_0^2/b^2)) = C_{ij,N}(\alpha_s(Q^2)) e^{[\alpha_s(\mu_R^2) C_{ij,N}^{(1)} / 2\pi] \lambda / (1-\lambda)}$ to the corrections down by $\alpha_s(\mu_R^2)$, for the N -th moment of the coefficient function of (7), so that we make the replacement $C_{ij,N}(\alpha_s(b_0^2/b^2)) \rightarrow C_{ij,N}(\alpha_s(Q^2)) = \delta_{ij} [1 + (\alpha_s(Q^2) C_F / 4\pi) (\pi^2 - 8)]$, up to the corrections of NNLL level for (12). Similarly, performing the large-logarithmic expansion for explicit formula of the NLO evolution operator $U_{ij,N}(b_0^2/b^2, Q^2)$, we find

$$U_{ij,N}(b_0^2/b^2, Q^2) = \delta_{ij} e^{R_N(\lambda)}, \quad R_N(\lambda) \equiv \frac{\Delta_T P_{qq,N}}{2\pi\beta_0} \ln(1 - \lambda), \quad (13)$$

up to the corrections down by $\alpha_s(\mu_R^2)$ which correspond to the NNLL terms when substituted into (12), (4). Here $\Delta_T P_{qq,N} = -2C_F[\psi(N+1) + \gamma_E - 3/4]$ is the N -th Mellin moment

of the LO DGLAP splitting function for the transversity. As a result, (12) is expressed as

$$\Delta_T X_{N_1, N_2}^{\text{NLL}}(Q_T^2, Q^2) = \left[1 + \frac{\alpha_s(Q^2)}{2\pi} C_F(\pi^2 - 8) \right] \delta H_{N_1, N_2}(Q^2) I_{N_1, N_2}(Q_T^2, Q^2), \quad (14)$$

$$I_{N_1, N_2}(Q_T^2, Q^2) \equiv \int_0^\infty db \frac{b}{2} J_0(bQ_T) e^{S(b, Q) + R_{N_1}(\lambda) + R_{N_2}(\lambda)}, \quad (15)$$

where $\delta H_{N_1, N_2}(Q^2)$ is the double Mellin-moments of $\delta H(x_1^0, x_2^0; Q^2)$ of (1), defined similarly as (12). The complete dependence on b is included in the exponential factor $e^{S(b, Q) + R_{N_1}(\lambda) + R_{N_2}(\lambda)}$ through $L = \ln(Q^2 b^2 / b_0^2)$, so that all-order resummation of the large logarithms L and the associated b -integral in (15) are now accomplished at the partonic level.

We also mention some other “reorganization”, which is explained in [6] and is necessary in order to treat properly too short and long distance involved in the b integration of (15): firstly, to treat too short distance $Qb \ll 1$, we make the replacement

$$L \rightarrow \tilde{L} = \ln(Q^2 b^2 / b_0^2 + 1), \quad (16)$$

in the definition (11) of λ , following [14]; note that the integrand of (15) depends on the large-logarithmic expansion parameter only through λ (see (8)-(10), (13)). This replacement allows us to reduce the unjustified large logarithmic contributions for $Qb \ll 1$, due to $L \gg 1$, as $\tilde{L} \rightarrow 0$ and $e^{S(b, Q) + R_{N_1}(\lambda) + R_{N_2}(\lambda)} \rightarrow 1$, while L and \tilde{L} are equivalent to organize the soft gluon resummation at small Q_T as $\tilde{L} = L + \mathcal{O}(1/(Qb)^2)$ for $Qb \gg 1$. Secondly, the functions (9) and (10) in the Sudakov exponent (8) are singular when $\lambda = \beta_0 \alpha_s(\mu_R^2) \tilde{L} \rightarrow 1$, and this singular behavior is related to the presence of the Landau pole in the perturbative running coupling $\alpha_s(\kappa^2)$ in QCD. To properly define the b integration of (15) for the corresponding long-distance region, it is necessary to specify a prescription to deal with this singularity [13]: decomposing the Bessel function in (15) into the two Hankel functions as $J_0(bQ_T) = (H_0^{(1)}(bQ_T) + H_0^{(2)}(bQ_T))/2$, we deform the b -integration contour for these two terms into upper and lower half plane in the complex b space, respectively, and obtain the two convergent integrals as $|b| \rightarrow \infty$. The new contour \mathcal{C} is taken as: from $b = 0$ to $b = b_c$ on the real axis, followed by the two branches, $b = b_c + e^{\pm i\theta} t$ with $t \in \{0, \infty\}$ and $0 < \theta < \pi/4$; a constant b_c is chosen as $0 \leq b_c < b_L$, where $b = b_L$ gives the solution for $\lambda = 1$. Note, this choice of contours is completely equivalent to the original contour, order-by-order in $\alpha_s(\mu_R^2)$, when the corresponding formulae are expanded in powers of α_s . Therefore, this contour deformation prescription provides us with a (formally) consistent definition of finite b -integral of (15) within a perturbative framework.

We now denote (14), with the replacement (16) and the new contour \mathcal{C} in (15), as $\Delta_T \tilde{X}_{N_1, N_2}^{\text{NLL}}(Q_T^2, Q^2)$, and also denote the double inverse Mellin transform of $\Delta_T \tilde{X}_{N_1, N_2}^{\text{NLL}}(Q_T^2, Q^2)$, from (N_1, N_2) space to (x_1^0, x_2^0) space, as $\Delta_T \tilde{X}^{\text{NLL}}(Q_T^2, Q^2, y)$. Defining (see (3))

$$\Delta_T \tilde{Y}(Q_T^2, Q^2, y) \equiv \Delta_T X(Q_T^2, Q^2, y) + \Delta_T Y(Q_T^2, Q^2, y) - \Delta_T \tilde{X}^{\text{NLL}}(Q_T^2, Q^2, y) \Big|_{\text{FO}}, \quad (17)$$

where $\Delta_T \tilde{X}^{\text{NLL}}(Q_T^2, Q^2, y)|_{\text{FO}}$ denotes the terms resulting from the expansion of the resummed expression up to the fixed-order $\alpha_s(\mu_R^2)$, we obtain the final form of our differential

cross section for tDY with the soft gluon resummation as [6]

$$\frac{\Delta_T d\sigma}{dQ^2 dQ_T^2 dy d\phi} = \cos(2\phi) \frac{\alpha^2}{3 N_c S Q^2} \left[\Delta_T \tilde{X}^{\text{NLL}}(Q_T^2, Q^2, y) + \Delta_T \tilde{Y}(Q_T^2, Q^2, y) \right]. \quad (18)$$

From the derivation explained above, the expansion of this cross section in powers of $\alpha_s(\mu_R^2)$ fully reproduces the first three towers of logarithms, $\alpha_s^n \ln^m(Q^2/Q_T^2)/Q_T^2$ with $m = 2n - 1, 2n - 2$ and $2n - 3$, associated with the soft-gluon emission for small Q_T ($\ll Q$), and also coincides exactly with the fixed-order result (3) to $\mathcal{O}(\alpha_s)$. Therefore, this formula (18) avoids any double counting over the entire range of Q_T . Note that $\Delta_T \tilde{Y}(Q_T^2, Q^2, y)$ of (17) corresponds to the “modified finite component” in our resummation framework: because the first and the third terms in the RHS of (17) cancel with each other for $Q_T \ll Q$, $\Delta_T \tilde{Y}(Q_T^2, Q^2, y)$ is less singular as $Q_T \rightarrow 0$ than $Q_T^{-2} \times (\ln(Q^2/Q_T^2) \text{ or } 1)$ or $\delta(Q_T^2)$, see the discussion below (3). Combined with $\Delta_T X^{(0)} \propto \delta(Q_T^2)$, this also implies that $\Delta_T \tilde{Y}(Q_T^2, Q^2, y)$ is of order $\alpha_s(\mu_R^2)$. In fact, (17) coincides exactly with $\Delta_T Y(Q_T^2, Q^2, y)$ if (16) is not performed.

Because of this “regular” behavior of $\Delta_T \tilde{Y}(Q_T^2, Q^2, y)$ as $Q_T \rightarrow 0$, we may consider (17) as the definition for the region where $Q_T > 0$; in this case, the first two terms correspond to (3) for $Q_T > 0$, i.e.,

$$\frac{\Delta_T d\sigma^{\text{LO}}}{dQ^2 dQ_T^2 dy d\phi} = \cos(2\phi) \frac{\alpha^2}{3 N_c S Q^2} \left[\Delta_T X^{(1)}(Q_T^2, Q^2, y) \Big|_{Q_T^2 > 0} + \Delta_T Y(Q_T^2, Q^2, y) \right], \quad (19)$$

which gives the formula for the LO QCD prediction of tDY at the large- Q_T region. Therefore, our formula (18) is actually the NLL resummed part, with the contributions to $\mathcal{O}(\alpha_s)$ (the third term of (17)) subtracted, plus the LO cross section; we refer to (18) as the “NLL+LO” prediction, which gives the well-defined tDY differential cross section in the $\overline{\text{MS}}$ scheme over the entire range of Q_T . It is straightforward to see that the integral of (18) over Q_T reproduces that of (3) exactly, because $\tilde{L} = 0$ at $b = 0$ (see also [14]).

We can extend the above results to unpolarized DY by mostly trivial substitutions to switch from spin-dependent quantities to spin-averaged ones, e.g., by removing “ Δ_T ” and making the replacement, $\delta H(x_1, x_2; \mu^2) \rightarrow H(x_1, x_2; \mu^2)$, $\cos(2\phi)\alpha^2/(3N_c S Q^2) \rightarrow 2\alpha^2/(3N_c S Q^2)$, etc., in the above relevant formulae. The explicit form of the spin-averaged quantities, such as $X(Q_T^2, Q^2, y)$, $Y(Q_T^2, Q^2, y)$, as well as those corresponding to the coefficient functions $C_{ij}(z, \alpha_s)$ in (4), can be obtained from the results in [15, 18]. A different point from the polarized case is that now the gluon distribution $f_g(x, \mu^2) \equiv g(x, \mu^2)$ participates, so that the suffix i, j of the “spin-averaged $C_{ij}(z, \alpha_s)$ ” can be “ g ” as well as “ q, \bar{q} ”. This also implies that $\Delta_T P_{qq, N}$ appearing in (13) has to be replaced by the Mellin moment of the LO DGLAP splitting functions for the unpolarized case, which involve the mixing of gluon, and the “new $U_{ij, N}(b_0^2/b^2, Q^2)$ ” represent the corresponding “evolution matrix” that was discussed in [14, 13]. On the other hand, the formulae (8)-(10) of the Sudakov exponent hold also for the unpolarized case, reflecting that the coefficients (6) relevant at the NLL level are universal [11, 12, 13, 14]. We list explicit form of the relevant formulae for the unpolarized cross sections in Appendix.

Taking the ratio of (18) to the corresponding NLL+LO prediction for unpolarized differential cross section, we obtain the double transverse-spin asymmetry in tDY, for transverse-momentum Q_T , invariant-mass Q , and rapidity y of the produced lepton pair, and azimuthal angle ϕ of one of the leptons, as

$$\mathcal{A}_{TT}(Q_T) = \frac{1}{2} \cos(2\phi) \frac{\Delta_T \tilde{X}^{\text{NLL}}(Q_T^2, Q^2, y) + \Delta_T \tilde{Y}(Q_T^2, Q^2, y)}{\tilde{X}^{\text{NLL}}(Q_T^2, Q^2, y) + \tilde{Y}(Q_T^2, Q^2, y)}. \quad (20)$$

To the fixed-order α_s without the soft gluon resummation, (20) reduces to the LO prediction of the asymmetry for $Q_T > 0$,

$$\mathcal{A}_{TT}^{\text{LO}}(Q_T) = \frac{1}{2} \cos(2\phi) \frac{\Delta_T X^{(1)}(Q_T^2, Q^2, y)|_{Q_T^2 > 0} + \Delta_T Y(Q_T^2, Q^2, y)}{X^{(1)}(Q_T^2, Q^2, y)|_{Q_T^2 > 0} + Y(Q_T^2, Q^2, y)}, \quad (21)$$

as the ratio of (19) to the corresponding unpolarized cross section.

3 The asymmetries $\mathcal{A}_{TT}(Q_T)$ at RHIC and J-PARC

We evaluate the asymmetries, derived in the last section, as a function of Q_T . We use the similar parton distributions as in the previous NLO studies [4] of Q_T -independent A_{TT} of (2): for the transversity $\delta q(x, Q^2)$ participating in the numerator of the asymmetries, we use a model of the NLO transversity distributions, which obey the corresponding NLO DGLAP evolution equation and are assumed to saturate the Soffer bound [19] as $\delta q(x, \mu_0^2) = [q(x, \mu_0^2) + \Delta q(x, \mu_0^2)]/2$ at a low input scale $\mu_0 \simeq 0.6$ GeV using the NLO GRV98 [20] and GRSV2000 (“standard scenario”) [21] distributions $q(x, \mu_0^2)$ and $\Delta q(x, \mu_0^2)$, respectively. The NLO GRV98 distributions $q(x, Q^2), g(x, Q^2)$ are also used for calculating the unpolarized cross sections in the denominator of the asymmetries.

It is known that the Q_T -spectrum of DY lepton pair is affected by another nonperturbative effects, which become important for small Q_T region [15]: we have obtained the well-defined tDY cross sections and asymmetries that are free from any singularities, with a consistent definition of the integration in (15) over the whole b region. However, the integrand of (15) involving purely perturbative quantities is not accurate for extremely large $|b|$ region in QCD, and the corresponding long-distance behavior has to be complemented by the relevant nonperturbative effects. Formally those nonperturbative effects play role to compensate the ambiguity that the prescription for the b integration in (15) to avoid the singularity in the Sudakov exponent $S(b, Q)$ of (8)-(10) is actually not unique (see [15]). Therefore, following [15, 13, 14], we make the replacement in (15) as

$$e^{S(b, Q)} \rightarrow e^{S(b, Q) - g_{NP} b^2}, \quad (22)$$

with a nonperturbative parameter g_{NP} . Because exactly the same Sudakov factor $e^{S(b, Q)}$ participates in the corresponding formula for the unpolarized case as noted above (20), we perform the replacement (22) with the same nonperturbative parameter g_{NP} in the

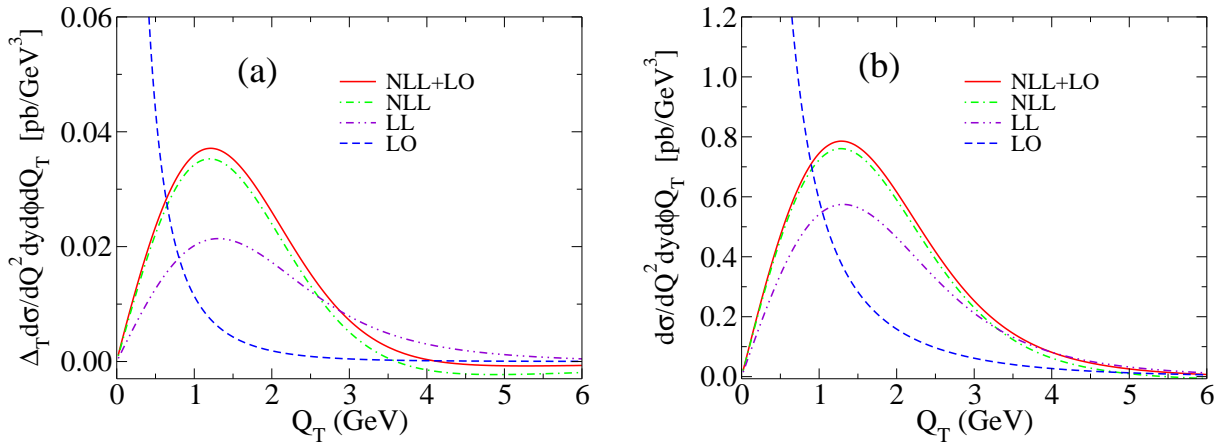


Figure 1: The spin-dependent and spin-averaged differential cross sections for tDY: (a) $\Delta_T d\sigma/dQ^2 dQ_T dy d\phi$ and (b) $d\sigma/dQ^2 dQ_T dy d\phi$, as a function of Q_T at RHIC kinematics, $\sqrt{S} = 200$ GeV, $Q = 5$ GeV, $y = 2$ and $\phi = 0$, with $g_{NP} = 0.5$ GeV 2 .

NLL+LO unpolarized differential cross section contributing to the denominator of (20). This may be interpreted as assuming the same “intrinsic transverse momentum” of partons inside nucleon for both polarized and unpolarized cases, corresponding to the Gaussian smearing factor of (22). We use $g_{NP} \simeq 0.5$ GeV 2 , suggested by the study of the Q_T -spectrum in unpolarized case [22].

For all the following numerical evaluations, we choose $\phi = 0$ for the azimuthal angle of one lepton, $\mu_F = \mu_R = Q$ for the factorization and renormalization scales and $b_c = 0$, $\theta = \frac{7}{32}\pi$ for the integration contour \mathcal{C} explained below (16).

First of all, we present the transverse-momentum Q_T -spectrum of the DY lepton pair for $\sqrt{S} = 200$ GeV, $Q = 5$ GeV, and $y = 2$, which correspond to the detection of dileptons with the PHENIX detector at RHIC. The solid curve in Fig. 1(a) shows the NLL+LO differential cross section (18) for tDY, multiplied by $2Q_T$, with $g_{NP} = 0.5$ GeV 2 for (22). We also show the contribution from the NLL resummed component $\Delta_T \tilde{X}^{\text{NLL}}$ in (18) by the dot-dashed curve, and the LO result using (19) by the dashed curve. Fig. 1(b) is same as Fig. 1(a) but for the unpolarized differential cross sections. The LO results become large and diverge as $Q_T \rightarrow 0$, while the NLL+LO results are finite and well-behaved over all regions of Q_T . The soft gluon resummation gives dominant contribution around the peak of the solid curve, i.e., at intermediate Q_T as well as small Q_T . To demonstrate the resummation effects in detail, the two-dot-dashed curves in Figs. 1(a), (b) show the LL result which is obtained from the corresponding NLL result (dot-dashed curve) by omitting the contributions corresponding to the NLL level, i.e., $h^{(1)}(\lambda)$, $R_{N_1}(\lambda)$, $R_{N_2}(\lambda)$ in (15) and $\alpha_s(Q^2)C_F(\pi^2 - 8)/2\pi$ in (14) for the polarized case (see (8) and the discussion below (11)), and similarly for the unpolarized case. The LL contributions are sufficient for obtaining the finite cross section, causing considerable suppression in the small Q_T region. On the other hand, it is remarkable that the contributions at the NLL level provide significant enhancement from the LL result,

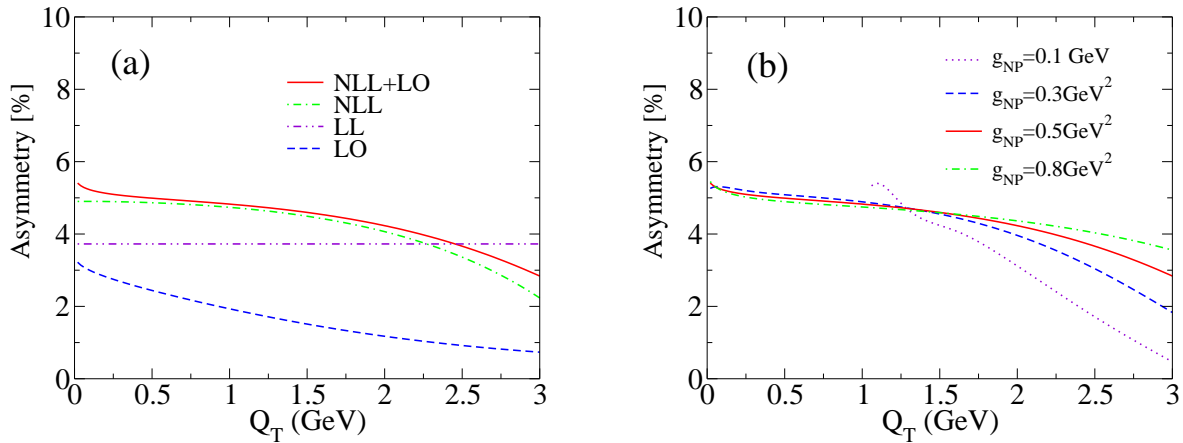


Figure 2: The asymmetries $\mathcal{A}_{TT}(Q_T)$ at RHIC kinematics, $\sqrt{S} = 200$ GeV, $Q = 5$ GeV, $y = 2$ and $\phi = 0$: (a) $\mathcal{A}_{TT}(Q_T)$ obtained from each curve in Fig. 1. (b) The NLL+LO $\mathcal{A}_{TT}(Q_T)$ of (20) with (22) using various values for g_{NP} .

around the peak region for both polarized and unpolarized cases, and the effect is more pronounced for the former. Among the relevant NLL contributions, the “universal” term $h^{(1)}(\lambda)$ produces similar (enhancement) effect for both (a) and (b) of Fig. 1, while the other NLL contributions, associated with the evolution operators and the $\mathcal{O}(\alpha_s(Q^2))$ coefficient functions (see e.g. (13), (14)), give different effects to the polarized and unpolarized cases.

Fig. 2(a) shows the double transverse-spin asymmetries in the small Q_T region for tDY at RHIC, obtained as the ratio of the results in Fig. 1(a) to the corresponding results in Fig. 1(b) for respective lines, so that the solid curve gives the NLL+LO result (20), the dot-dashed curve shows the NLL result,

$$\mathcal{A}_{TT}^{\text{NLL}}(Q_T) = \frac{1}{2} \cos(2\phi) \frac{\Delta_T \tilde{X}^{\text{NLL}}(Q_T^2, Q^2, y)}{\tilde{X}^{\text{NLL}}(Q_T^2, Q^2, y)} , \quad (23)$$

and the dashed curve shows the LO result (21). The NLL+LO result is almost flat for $Q_T \rightarrow 0$ as well as around the peak region of the NLL+LO cross section in Fig. 1. This flat behavior is dominated by the NLL resummed components, and reflects the fact that the soft gluon emission effects resummed into the Sudakov factor $e^{S(b,Q)}$ with (8) are universal to the NLL accuracy between the numerator and denominator of (20). Slight increase of the solid line for $Q_T \rightarrow 0$ is due to the terms $\propto \ln(Q^2/Q_T^2)$ contained in the “regular components” $\Delta_T \tilde{Y}$ and \tilde{Y} in (20) (see (17)), but such weak singularities which show up only at very small Q_T will be irrelevant for most practical purposes. The LO result, obtained as the ratio of the two LO curves divergent as $Q_T \rightarrow 0$ in Figs. 1(a) and (b), gives the finite asymmetry for $Q_T > 0$, but it does not have the flat behavior, i.e., decreases for increasing Q_T , and is much smaller than the NLL+LO result. On the other hand, we note that the LL result, retaining only the resummed components corresponding to the LL level, is given by (see

(14), (15))

$$\mathcal{A}_{TT}^{\text{LL}}(Q_T) = \frac{1}{2} \cos(2\phi) \frac{\delta H(x_1^0, x_2^0; Q^2)}{H(x_1^0, x_2^0; Q^2)} \approx A_{TT} , \quad (24)$$

which is independent of Q_T , because the Q_T -dependent factor (15) with $S(b, Q) + R_{N_1}(\lambda) + R_{N_2}(\lambda) \rightarrow h^{(0)}(\lambda)/\alpha_s(Q^2)$ is common for both polarized and unpolarized cases. Namely the LL resummation effects cancel exactly between the numerator and the denominator in the asymmetry (24). As indicated in (24), the resulting value shown by the two-dot-dashed curve in Fig. 2(a) coincides with the Q_T -independent asymmetry (2) up to the NLO QCD corrections; note that $A_{TT} = 4.0\%$ including the NLO corrections similarly as [4] (see Table 1 below). However, we recognize that the soft-gluon resummation contributions at the NLL level enhances the asymmetry at the small Q_T -region significantly, compared with the LL or fixed-order result. This is caused by the enhancement of the cross sections in Fig. 1 discussed above, due to the universal $h^{(1)}(\lambda)$ term and the other spin-dependent contributions. In particular, the evolution operators like (13) in the latter contributions allow the participation of the parton distributions at the scale $b_0/b \sim Q_T$, and the components associated with those parton distributions indeed play dominant roles due to the mechanism embodied by the Sudakov factor $e^{S(b, Q)}$ of (15). Combined with the different x -dependence between the transversity and density distributions as noted in (ii) above, the resulting enhancement arises differently between (a) and (b) in Fig. 1, and enhances the asymmetry as in Fig. 2(a).

In Fig. 2(b) we show the NLL+LO asymmetries $\mathcal{A}_{TT}(Q_T)$ of (20), with (22) using various values of g_{NP} . Here the solid curve is the same as the solid curve in Fig. 2(a), using $g_{NP} = 0.5 \text{ GeV}^2$. The result demonstrates that our NLL+LO asymmetry in the relevant small- Q_T region is almost independent of the value of g_{NP} in the range $g_{NP} = 0.3\text{-}0.8 \text{ GeV}^2$. Although, at RHIC kinematics, the Q_T -spectrum from the spin-dependent cross section (18) with (22) receives a sizable smearing effect in the relevant small- Q_T region [6], the corresponding g_{NP} -dependence is canceled by the similar dependence of the unpolarized cross section in the asymmetry (20). In our framework, such cancellation of the g_{NP} -dependence between the numerator and the denominator of (20) is observed for all relevant kinematics of our interest at RHIC, and also at J-PARC discussed below. However, we mention that too small value of g_{NP} is useless in practice: the Gaussian smearing factor of (22) for $g_{NP} = 0.1 \text{ GeV}^2$ is insufficient to suppress sensitivity to the extremely large $|b|$ region in (15), so that the b integration receives the “inaccurate” long-distance perturbative contributions considerably at small Q_T , which lead to unstable numerical behavior for $Q_T \lesssim 1 \text{ GeV}$. For all the following calculations, we use $g_{NP} = 0.5 \text{ GeV}^2$.

Fig. 3 shows the NLL+LO asymmetries $\mathcal{A}_{TT}(Q_T)$ of (20) at RHIC kinematics, $\sqrt{S} = 200 \text{ GeV}$ and various values of the dilepton invariant mass Q , using $y = 2$ and $y = 0$ for (a) and (b), respectively; the dashed curve in (a) is the same as the solid curve in Figs. 2(a), (b). For all cases in Fig. 3, we observe the typical flat behavior of $\mathcal{A}_{TT}(Q_T)$ in the small Q_T region, similarly as Fig. 2. On the other hand, $\mathcal{A}_{TT}(Q_T)$ increases for increasing Q , and the value in the flat region reaches about 10% for $Q = 20 \text{ GeV}$ in Fig. 3(a). Such dependence on Q is associated with the small- x behavior of the relevant parton distributions: smaller Q corresponds to smaller $x_{1,2}^0 = e^{\pm y} Q / \sqrt{S}$, so that the small- x rise of the unpolarized sea-distributions enhances the denominator of (20). We obtain larger $\mathcal{A}_{TT}(Q_T)$ for $y = 2$

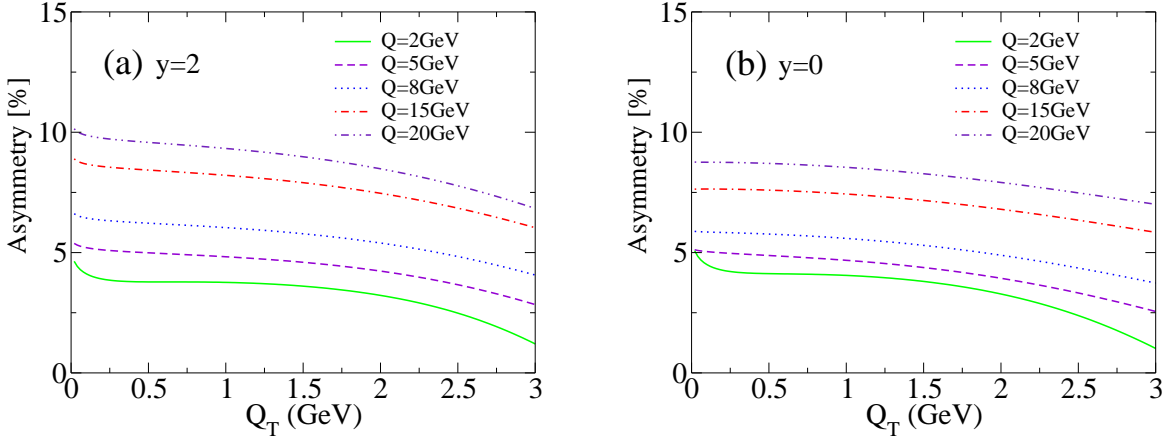


Figure 3: The NLL+LO $\mathcal{A}_{TT}(Q_T)$ of (20) with (22) using $g_{NP} = 0.5$ GeV 2 at RHIC kinematics, $\sqrt{S} = 200$ GeV, $\phi = 0$ with $y = 2$ and $y = 0$ for (a) and (b), respectively.

		$Q = 2\text{GeV}$	$Q = 5\text{GeV}$	$Q = 8\text{GeV}$	$Q = 15\text{GeV}$	$Q = 20\text{GeV}$
$\sqrt{S} = 200\text{GeV}$	$y = 2$	3.3%	4.0%	4.9%	6.5%	7.4%
	$y = 0$	3.5%	3.7%	4.4%	5.9%	6.9%
$\sqrt{S} = 500\text{GeV}$	$y = 2$	1.8%	2.0%	2.4%	3.4%	4.0%
	$y = 0$	2.2%	2.1%	2.4%	3.2%	3.8%

Table 1: The Q_T -independent asymmetry A_{TT} of (2) including the NLO QCD corrections at RHIC kinematics.

compared with the $y = 0$ case, but the y -dependence of $\mathcal{A}_{TT}(Q_T)$ is not so strong for all Q . For comparison, we also evaluate the Q_T -independent asymmetry A_{TT} of (2) including the NLO QCD corrections and with the same nonperturbative inputs as those used in Fig. 3. The results are shown in Table 1, and these exhibit similar behavior with respect to the Q and y dependence as that in Fig. 3. Note that we reproduce the NLO value of A_{TT} in Table 1 when we integrate respectively the numerator and the denominator of the NLL+LO asymmetry (20) over Q_T for each curve of Fig. 3 (see discussion below (19)). But the NLO A_{TT} are smaller by about 20% than the corresponding values of the NLL+LO $\mathcal{A}_{TT}(Q_T)$ in the “flat” region at small Q_T . This enhancement of $\mathcal{A}_{TT}(Q_T)$ compared with A_{TT} arises from the soft gluon resummation at the NLL level, as discussed in Fig. 2(a) above.

Fig. 4 is same as Fig. 3, but for another RHIC kinematics with $\sqrt{S} = 500$ GeV. General behavior for the Q_T , Q and y dependence is similar as that in Fig. 3. Comparing the curves with the same values of Q , y between Figs. 3 and 4, $\mathcal{A}_{TT}(Q_T)$ are smaller for higher energy $\sqrt{S} = 500$ GeV than those for $\sqrt{S} = 200$ GeV. This reflects the smaller $x_{1,2}^0 = e^{\pm y}Q/\sqrt{S}$ for larger \sqrt{S} , and the corresponding enhancement of the denominator in (20). Similarly as Fig. 3, the NLL+LO $\mathcal{A}_{TT}(Q_T)$ in the flat region of Fig. 4 are larger by 20-30% than the corresponding NLO A_{TT} shown in Table 1. It is generally true, regardless of the

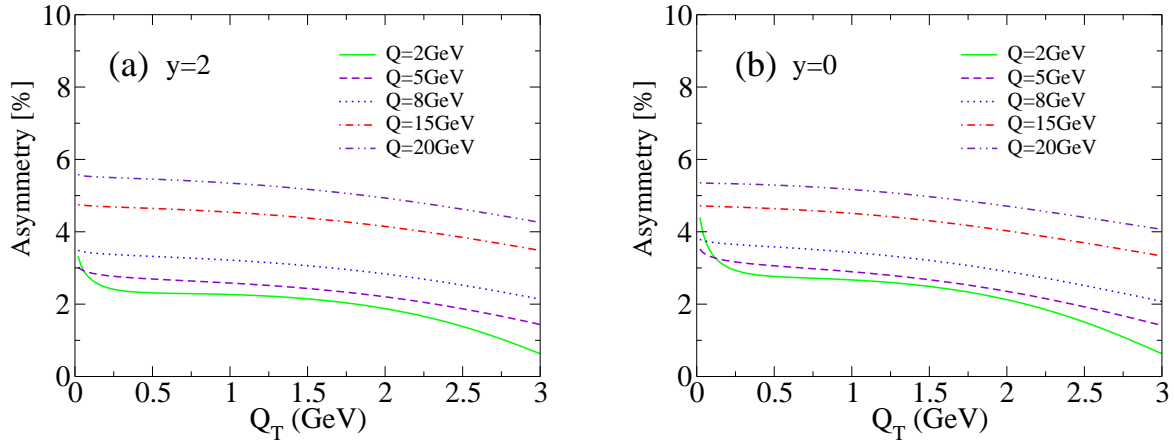


Figure 4: Same as Fig. 3, but for $\sqrt{S} = 500$ GeV.

specific kinematics or the detailed behavior of nonperturbative inputs, that the NLL+LO $\mathcal{A}_{TT}(Q_T)$ of (20) in the flat region is considerably larger than the corresponding NLO A_{TT} , because this phenomenon is mainly governed by the partonic mechanism associated with the soft gluon resummation at the NLL level, as demonstrated in Figs. 1, 2. On the other hand, apparently the absolute magnitude of both $\mathcal{A}_{TT}(Q_T)$ and A_{TT} is influenced by the detailed behavior of the input parton distributions, in particular, by their small- x behavior at RHIC. For example, if we change the input parton distributions, explained above (22), from the NLO GRV98 and GRSV2000 distributions into the NLO GRV94 [23] and GRSV96 [24] distributions, the NLO values of A_{TT} become smaller by 30-40% than the corresponding values in Table 1. We note that the latter distributions are the ones used in the calculation of [4], and the small- x behavior of the transversity distributions, resulting from $\delta q(x, \mu_0^2) = [q(x, \mu_0^2) + \Delta q(x, \mu_0^2)]/2$ at the input scale μ_0 , is rather different between those two choices of the distributions, reflecting that the helicity distributions at small x are still poorly determined from experiments. [§]

Next we discuss tDY foreseen at J-PARC. Fig. 5(a) shows the Q_T spectrum of the produced lepton pair for J-PARC kinematics, $\sqrt{S} = 10$ GeV, $Q = 2$ GeV and $y = 0$. The curves show the spin-dependent differential cross sections, and have the same meaning as the corresponding curves in Fig. 1(a). The double transverse-spin asymmetries are obtained as the ratio of the results in Fig. 5(a) to the corresponding results for the unpolarized differential cross sections, as shown in Fig. 5(b). We see that the results at J-PARC obey the similar pattern as those at RHIC shown in Figs. 1, 2: the flat behavior is observed for the NLL+LO $\mathcal{A}_{TT}(Q_T)$ at $Q_T \rightarrow 0$ as well as around the peak region of the NLL+LO cross section, and this is dominated by the NLL resummed components. Also the soft-gluon resummation contributions at the NLL level enhances the asymmetry at the small Q_T -region significantly, compared with the LL of (24) or the fixed-order LO result. As a

[§] We thank H. Yokoya and W. Vogelsang for clarifying this point.

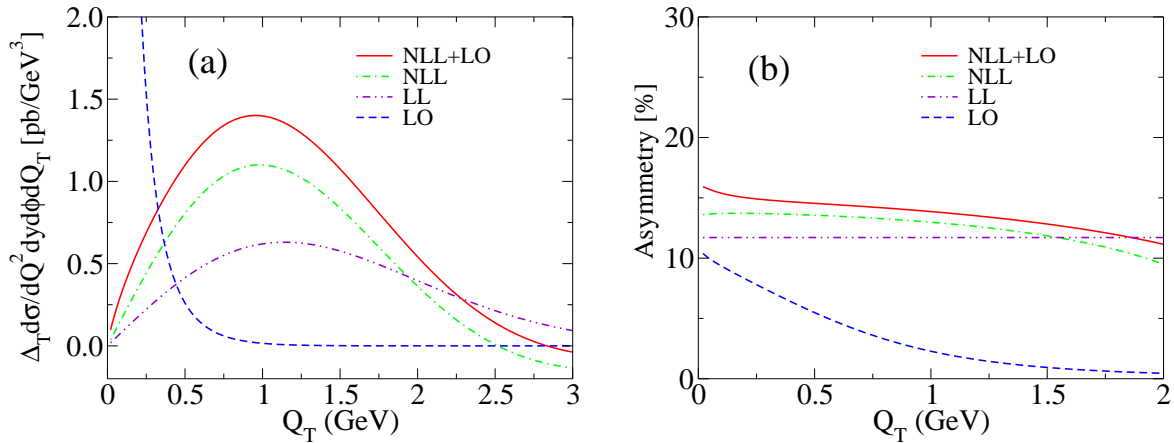


Figure 5: The tDY at J-PARC kinematics, $\sqrt{S} = 10$ GeV, $Q = 2$ GeV, $y = 0$ and $\phi = 0$. (a) The spin-dependent differential cross section $\Delta_T d\sigma/dQ^2 dQ_T dy d\phi$ using $g_{NP} = 0.5$ GeV². (b) The asymmetries $\mathcal{A}_{TT}(Q_T)$ obtained by using each curve in (a).

		$Q = 2$ GeV	$Q = 2.5$ GeV	$Q = 3.5$ GeV
$\sqrt{S} = 10$ GeV	$y = 0$	12.8%	12.9%	12.5%
	$y = 0.5$	13.9%	14.8%	15.9%

Table 2: Same as Table 1 but for J-PARC kinematics.

result, we get $\mathcal{A}_{TT}(Q_T) \simeq 15\%$ as the NLL+LO prediction around the flat region, which should be compared with the corresponding prediction $A_{TT} = 12.8\%$ for (2) including the NLO corrections (see Table 2). The reason why we obtain much larger values of $\mathcal{A}_{TT}(Q_T)$, and also of A_{TT} , than the RHIC case is the larger $x_{1,2}^0 = 0.2$ probed at J-PARC, where the transversities are larger and the unpolarized sea distributions are smaller. Another difference compared with the RHIC case is that the contribution of the “regular component” $\Delta_T \tilde{Y}$ of (17) in Fig. 5(a), and the associated increase of the solid curve as $Q_T \rightarrow 0$ in Fig. 5(b), due to the terms $\propto \ln(Q^2/Q_T^2)$ in $\Delta_T \tilde{Y}$ and \tilde{Y} of (20), are more pronounced, but the latter effect shows up only for $Q_T \lesssim 0.5$ GeV.

In Fig. 6 we show the NLL+LO asymmetries $\mathcal{A}_{TT}(Q_T)$ of (20) at J-PARC kinematics, $\sqrt{S} = 10$ GeV and various values of Q , with $y = 0$ and $y = 0.5$ for (a) and (b), respectively; the solid curve in (a) is the same as the solid curve in Fig. 5(b). We observe the flat behavior of $\mathcal{A}_{TT}(Q_T)$ in the small Q_T region, where $\mathcal{A}_{TT}(Q_T) \simeq 15\text{-}20\%$ and these values are significantly larger than the corresponding results for the Q_T -independent, NLO asymmetry A_{TT} of (2), shown in Table 2. We note that the dependence of $\mathcal{A}_{TT}(Q_T)$, as well as A_{TT} , on Q is weak in contrast to the RHIC case; recall that the rather strong Q -dependence in Figs. 3, 4 was induced mainly by the growth of the unpolarized sea-distributions for the small $x_{1,2}^0$, probed at RHIC.

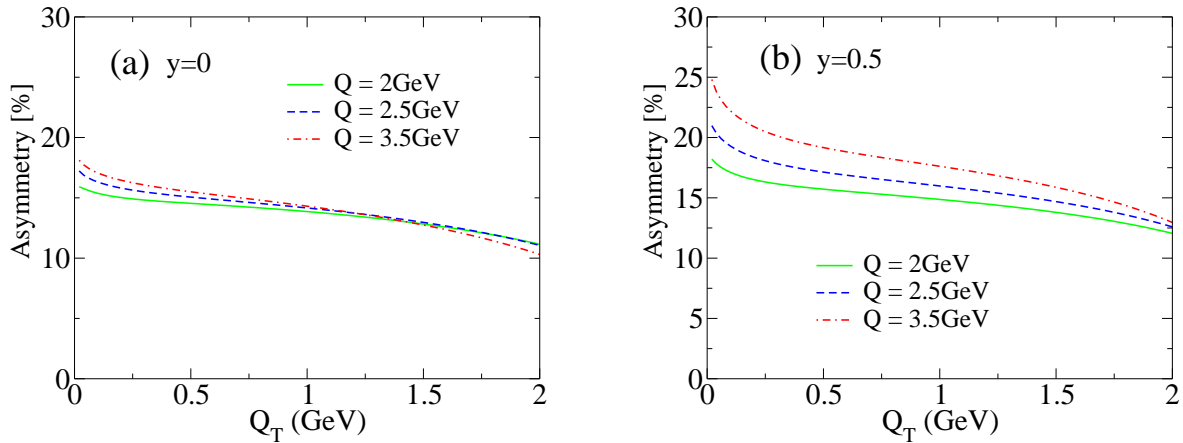


Figure 6: The NLL+LO $\mathcal{A}_{TT}(Q_T)$ of (20) with (22) using $g_{NP} = 0.5$ GeV² at J-PARC kinematics, $\sqrt{S} = 10$ GeV, $\phi = 0$ with $y = 0$ and $y = 0.5$ for (a) and (b), respectively.

4 The saddle point formula

In Sec. 3, we have observed the universal flat behavior of NLL+LO $\mathcal{A}_{TT}(Q_T)$ of (20) at small Q_T , including the region around the peak of each DY cross section in the numerator and denominator of (20) for both RHIC and J-PARC cases. We have also demonstrated in Figs. 2 and 5 that those flat behavior is driven by the dominant effects from soft gluon resummation embodied by the NLL resummed components $\Delta_T \tilde{X}^{\text{NLL}}$ and \tilde{X}^{NLL} in (20). As a result, the values of $\mathcal{A}_{TT}(Q_T)$ obtained in the “flat region” of the corresponding experimental data may be compared, to a good accuracy, with (23). Still, extraction of transversity distributions through such analysis should be a complicated task compared with the usual fixed-order analysis: in the flat region of $\mathcal{A}_{TT}(Q_T)$, the b integration in the resummed part (4) (see also (14), (15)) mixes up the parton distributions numerically with very large perturbative effects due to the Sudakov factor shown in Figs. 1 and 5, as well as with another nonperturbative effects associated with g_{NP} of (22). Thus in each of the numerator and the denominator of (20), the information on the parton distributions is associated with a portion of the large numerical quantity whose major part would cancel in the ratio of (20), and this fact would obscure the straightforward extraction of the transversity using the above formulae like (14), (15), in particular with respect to its accuracy.

We are able to derive a simple analytic formula which allows more direct extraction of the transversity distributions from the experimental data in the flat region of $\mathcal{A}_{TT}(Q_T)$ and also clarifies the accuracy of the resulting distributions. For this purpose, we first note that the extrapolation of $\mathcal{A}_{TT}(Q_T)$ in the flat region to $Q_T = 0$ corresponds to the case without the (experimentally uninteresting) weak enhancement at very small Q_T due to the terms $\propto \log(Q^2/Q_T^2)$ in the regular components $\Delta_T \tilde{Y}$ and \tilde{Y} of (20), so that the resulting value is very close to the $Q_T \rightarrow 0$ limit of (23) in both RHIC and J-PARC cases (see Figs. 2-6). Namely, $\mathcal{A}_{TT}^{\text{NLL}}(Q_T = 0)$ may be considered to give a practical estimate of the data of

$\mathcal{A}_{TT}(Q_T)$ in the flat region with a good accuracy. Then, at $Q_T = 0$, the region $|b| \sim 1/\Lambda_{\text{QCD}}$ becomes important for the b integration of the relevant resummation formula (15). Note that we can treat “safely” such long-distance region, corresponding to the boundary of perturbative and nonperturbative physics, owing to that the nonperturbative smearing (22) suppresses the too long-distance region $|b| \gg 1/\Lambda_{\text{QCD}}$, and that the dependence on a specific choice of g_{NP} cancels in the asymmetries $\mathcal{A}_{TT}^{\text{NLL}}(Q_T = 0)$ as demonstrated in Fig. 2(b) (see also (30) below).

For simplicity in the presentation, we fix as $\mu_R = Q$ in the following. In the relevant region $|b| \sim 1/\Lambda_{\text{QCD}}$, we have $|\tilde{L}| \sim \ln(Q^2/\Lambda_{\text{QCD}}^2) \sim 1/\alpha_s(Q^2)$, i.e., $|\lambda| \sim 1$ (see (16), (11)). Because all logarithms, \tilde{L} and $\ln(Q^2/\Lambda_{\text{QCD}}^2)$, are counted equally large for $Q \gg \Lambda_{\text{QCD}}$, the resulting contributions to (15) are organized in terms of a single small parameter, $\alpha_s(Q^2)$, but with a different classification of the contributions in the order of $\alpha_s(Q^2)$ from the usual perturbation theory that can be used in an other region, $0 \leq |b| \lesssim 1/Q$: as discussed below (11), when $\lambda = \mathcal{O}(1)$, the NLL contributions in the Sudakov exponent (8) produce the $\mathcal{O}(1)$ effects in the resummation formula (15), while the NNLL contributions could yield the corrections of $\mathcal{O}(\alpha_s(Q^2))$. Therefore, when the region $|b| \sim 1/\Lambda_{\text{QCD}}$ is relevant as $Q_T \rightarrow 0$ and we neglect the NNLL contributions in (15), the other contributions that correspond to the same order of $\alpha_s(Q^2)$ in (14) should be neglected for a consistent treatment, as $[1 + \alpha_s(Q^2)C_F(\pi^2 - 8)/2\pi] \rightarrow 1$, so that ¶

$$\Delta_T X_{N_1, N_2}^{\text{NLL}}(Q_T^2 = 0, Q^2) = \delta H_{N_1, N_2}(Q^2) I_{N_1, N_2}(Q_T^2 = 0, Q^2). \quad (25)$$

We note that the contributions to the NLL resummation formula for the unpolarized case can be classified similarly in the $Q_T \rightarrow 0$ limit; in particular, the present classification implies that the gluon distributions decouple for $Q_T \rightarrow 0$ by negelecting the $\mathcal{O}(\alpha_s(Q^2))$ contributions of the corresponding coefficient functions C_{ij} (see (31) in Appendix).

It is also worth noting that this classification coincides with the “degree 0 approximation” discussed in [15]: in general, if one wants to evaluate the cross section for $Q_T \approx 0$ in an approximation where any corrections are suppressed by a factor of $[\ln(Q^2/\Lambda_{\text{QCD}}^2)]^{-(N+1)}$, one needs a “degree N ” approximation; i.e., for the perturbatively calculable functions in the general form of resummation formula (4) with (5), one needs A_q to order α_s^{N+2} , B_q to order α_s^{N+1} , C_{ij} to order α_s^N , and the β function to order α_s^{N+2} . This indicates that the NLL accuracy for a resummation formula corresponds to the degree 0 approximation when the region $Q_T \approx 0$ is considered. In particular, this implies that the $\mathcal{O}(\alpha_s)$ contribution in the coefficient function C_{ij} should be neglected for $Q_T \approx 0$; on the other hand, that contribution is necessary to ensure the NLL accuracy for $Q_T \gtrsim \Lambda_{\text{QCD}}$ in the classification based on resummed perturbation theory of towers of logarithms, $\alpha_s^n \ln^{2n-1}(Q^2/Q_T^2)/Q_T^2$, $\alpha_s^n \ln^{2n-2}(Q^2/Q_T^2)/Q_T^2$, and $\alpha_s^n \ln^{2n-3}(Q^2/Q_T^2)/Q_T^2$ [15, 14, 6].

Now we evaluate the b integral of (15) at $Q_T = 0$ according to the above classification. We have to use the exponentiated form in the integrand of (15) without Taylor expansion,

¶ In principle, we should use this classification also for the numerical calculations presented in Sec. 3 when $Q_T \approx 0$. But we did not make the corresponding replacement for the coefficient functions C_{ij} at $Q_T \approx 0$ in the calculations of Figs. 1-6. If we performed that replacement, the NLL+LO (20) as well as NLL (23) asymmetries at $Q_T \approx 0$ in those figures would increase by about 5%.

because the region $|\lambda| \sim 1$ is relevant (see (8)-(13)) [26]. This type of integrals can be evaluated with the saddle point method: we extend the saddle point evaluation applied to the LL resummation formula with $g_{NP} = 0$ [25, 15] into the case of our NLL resummation formula (15) with nonzero g_{NP} . The corresponding extension is possible based on the present formalism that accomplishes resummation at the partonic level. We note that previous saddle-point calculations consider the case with $g_{NP} = 0$ to avoid model dependence for the prediction of the cross sections, but the resultant saddle-point formula is applicable only to the production of extremely high-mass DY pair and is practically useless (see e.g. [25, 15, 27]). We find that, with nonzero g_{NP} , we can obtain a new saddle-point formula applicable to the RHIC and J-PARC cases; also, although the behavior of the cross sections are influenced by specific value of g_{NP} , the asymmetries are not, as already noted above.

When Q is large enough, $\alpha_s(Q^2) \ll 1$, so that the b integral in (15) with (22) and $Q_T = 0$ is dominated by a saddle point determined by mainly the LL term in the exponent (8) of the Sudakov form factor [25, 15]. In this case, the contributions to the b integration from too short ($|b| \ll 1/Q$) and long distance ($|b| \gg 1/\Lambda_{\text{QCD}}$) along the integration contour \mathcal{C} explained below (16) are exponentially suppressed: this allows us to give up the replacement (16); also we may neglect the integration along the two branches, $b = b_c + e^{\pm i\theta}t$ with $t \in \{0, \infty\}$, in \mathcal{C} , when b_c is sufficiently large but is less than the position of the singularity in the Sudakov exponent, b_L . In fact, we can check numerically that the relevant integrand has a nice saddle point well below b_L (above 0) for the kinematics of our interest. Then, changing the integration variable to λ , given by (11), we get (see (9), (10), (13))

$$I_{N_1, N_2}(Q_T^2 = 0, Q^2) = \frac{b_0^2}{4Q^2\beta_0\alpha_s(Q^2)} \int_{-\infty}^{\lambda_c} d\lambda e^{-\zeta(\lambda) + h^{(1)}(\lambda) + R_{N_1}(\lambda) + R_{N_2}(\lambda)}, \quad (26)$$

where $\lambda_c = \beta_0\alpha_s(Q^2) \ln(Q^2 b_c^2/b_0^2) (< 1)$, and

$$\zeta(\lambda) = -\frac{\lambda}{\beta_0\alpha_s(Q^2)} - \frac{h^{(0)}(\lambda)}{\alpha_s(Q^2)} + \frac{g_{NP}b_0^2}{Q^2} e^{\frac{\lambda}{\beta_0\alpha_s(Q^2)}}. \quad (27)$$

An important point is that the ratio, $[h^{(1)}(\lambda) + R_{N_1}(\lambda) + R_{N_2}(\lambda)]/\zeta(\lambda)$, actually behaves as a quantity of the order of $\alpha_s(Q^2)$ in the relevant region $0 < \lambda < \lambda_c$ of the integration in (26), even for nonzero $g_{NP} \simeq 0.5 \text{ GeV}^2$. The precise position of the saddle point in the integral of (26) is determined by the condition, $-\zeta'(\lambda) + h^{(1)'}(\lambda) + R_{N_1}'(\lambda) + R_{N_2}'(\lambda) = 0$, and we express its solution as $\lambda = \lambda_{SP} + \Delta\lambda_{SP}$ where λ_{SP} is the solution of $\zeta'(\lambda) = 0$, i.e.,

$$1 - \frac{A_q^{(1)}}{2\pi\beta_0} \frac{\lambda_{SP}}{1 - \lambda_{SP}} = \frac{g_{NP}b_0^2}{Q^2} e^{\frac{\lambda_{SP}}{\beta_0\alpha_s(Q^2)}} \quad (28)$$

is satisfied, and $\Delta\lambda_{SP} = [h^{(1)'}(\lambda_{SP}) + R_{N_1}'(\lambda_{SP}) + R_{N_2}'(\lambda_{SP})]/\zeta''(\lambda_{SP})$ denotes the shift of the saddle point at the NLL accuracy. Evaluating (26) around $\lambda = \lambda_{SP} + \Delta\lambda_{SP}$, we get

$$I_{N_1, N_2}(0, Q^2) = \left(\frac{b_0^2}{4Q^2\beta_0\alpha_s(Q^2)} \sqrt{\frac{2\pi}{\zeta''(\lambda_{SP})}} e^{-\zeta(\lambda_{SP}) + h^{(1)}(\lambda_{SP})} \right) e^{R_{N_1}(\lambda_{SP}) + R_{N_2}(\lambda_{SP})}, \quad (29)$$

to the NLL accuracy. Here the contributions from the third or higher order terms in the Taylor expansion of the exponent in (26) about the saddle point $\lambda = \lambda_{SP} + \Delta\lambda_{SP}$, as well as the other terms generated by the shift $\Delta\lambda_{SP}$, are found to give the effects behaving as $\mathcal{O}(\alpha_s(Q^2))$, i.e, are of the same order as the NNLL corrections, and thus are neglected, similarly as in (14), (25), according to the classification of the contributions at $Q_T = 0$. Substituting (29) into (25) and performing the double inverse Mellin transformation to the (x_1^0, x_2^0) space, the result is expressed as the factor in the parentheses of (29), multiplied by (1) with the scale, $\mu_F \rightarrow b_0/b_{SP}$ where $b_{SP} = (b_0/Q)e^{\lambda_{SP}/(2\beta_0\alpha_s(Q^2))}$, because $e^{R_{N_1}(\lambda_{SP})}$, $e^{R_{N_2}(\lambda_{SP})}$ in (29) can be identified with the NLO evolution operators from the scale Q to b_0/b_{SP} , to the present accuracy (see (13)). The saddle-point evaluation of the corresponding resummation formula for the unpolarized case can be performed similarly, and the result is given by the above result for the polarized case, with the replacement $\delta H(x_1^0, x_2^0; b_0^2/b_{SP}^2) \rightarrow H(x_1^0, x_2^0; b_0^2/b_{SP}^2)$. The common factor for both the polarized and unpolarized results, given by the contribution in the parentheses of (29), involves “very large perturbative effects” due to the Sudakov factor, and shows the well-known asymptotic behavior [25], $\sim (\Lambda_{\text{QCD}}^2/Q^2)^{a \ln(1+1/a)}$ with $a \equiv A_q^{(1)}/(2\pi\beta_0)$, for $Q \gg \Lambda_{\text{QCD}}$; but this factor cancels out for the asymmetry. As a result, we obtain the $Q_T \rightarrow 0$ limit of (23) as

$$\mathcal{A}_{TT}^{\text{NLL}}(Q_T = 0) = \frac{1}{2} \cos(2\phi) \frac{\delta H(x_1^0, x_2^0; b_0^2/b_{SP}^2)}{H(x_1^0, x_2^0; b_0^2/b_{SP}^2)}, \quad (30)$$

which is exact, up to the NNLL corrections corresponding to the $\mathcal{O}(\alpha_s(Q^2))$ effects. This remarkably compact formula is reminiscent of $\mathcal{A}_{TT}^{\text{LL}}(Q_T)$ of (24) that retains only the LL level resummation, or the Q_T independent asymmetry of (2), but is different in the scale of the parton distributions from those leading-order results. Namely, our result (30) demonstrates: in the $Q_T = 0$ limit, the all-order soft-gluon-resummation effects on the asymmetry mostly cancel between the numerator and the denominator of (30), but certain contributions at the NLL level survive the cancellation and are entirely absorbed into the unconventional scale b_0/b_{SP} for the relevant distribution functions.

The new scale b_0/b_{SP} is determined by solving (28) numerically, substituting $A_q^{(1)} = 2C_F$ from (6) and input values for Q and g_{NP} , but it is useful to consider its general behavior: the LHS of (28) equals 1 at $\lambda_{SP} = 0$, decreases as a concave function for increasing λ_{SP} , and vanishes at $\lambda_{SP} = 1/[1 + A_q^{(1)}/(2\pi\beta_0)] \cong 0.6$; while the RHS is in general much smaller than 1 at $\lambda_{SP} = 0$, increases as a convex function for increasing λ_{SP} , and is larger than 1 at $\lambda_{SP} \simeq 1$. Thus the solution of (28) corresponds to the case with $\text{LHS} = \text{RHS} \simeq 1/2$, more or less independently of the specific value of Q and g_{NP} , so that we get $b_0/b_{SP} \simeq b_0\sqrt{2g_{NP}}$. This result depends only mildly on the nonperturbative parameter g_{NP} , and suggests that one may always use $b_0/b_{SP} \simeq 1$ GeV, for the cases of our interest where Q is of several GeV and $g_{NP} \simeq 0.5$ GeV² as in Figs. 1-6. The actual numerical solution of (28) justifies this simple consideration at the level of 20% accuracy. This fact will be particularly helpful in the first attempt to compare (30) with the experimental data so as to extract the transversity distributions.

Our saddle-point formula (30) embodies the characteristic features of the NLL soft gluon resummation effects on the asymmetries $\mathcal{A}_{TT}(Q_T)$, emphasized in Sec. 3. In particular, our

derivation of (30) demonstrates clearly the mechanism, which makes the parton distributions at the low scale $\sim Q_T$ play dominant roles, and leads to the “enhancement” of the dot-dashed curve in Figs. 2 and 5. As noted in the beginning of this section, (30) may be directly compared with the experimental value of the asymmetries $\mathcal{A}_{TT}(Q_T)$, observed around the peak of the Q_T spectrum of the corresponding DY cross sections. But there is one caution for such application. As seen from the above derivation, the parton distributions appearing in (30) are the NLO distributions up to the corrections at the NNLL level; e.g., the transversity distributions appearing in the numerator of (30) is obtained by evolving the customary NLO transversity $\delta q(x, Q^2)$ at the scale Q , to the scale b_0/b_{SP} using (13) that is *the NLO evolution operators up to the NNLL corrections*. Therefore, the formula (30) can be used in the region where NNLL corrections are small; we know that the NNLL corrections at $Q_T \approx 0$ correspond to $\mathcal{O}(\alpha_s(Q^2))$ effects, and should be negligible in general. However, such straightforward estimate might fail at the edge region of the phase space, e.g., at the small x region: because the relevant evolution operators (13) actually coincide with the leading contributions in the large-logarithmic expansion of the usual LO DGLAP evolution,^{||} (30) would not accurate when the NLO corrections in the usual DGLAP evolution are large compared with the contributions of (13). Such situation would typically occur in the region with small $x_{1,2}^0$, corresponding to the case with large \sqrt{S} . In Table 3, we compare $\mathcal{A}_{TT}^{\text{NLL}}(Q_T = 0)$ using the numerical b -integration (“NB”), obtained as the $Q_T \rightarrow 0$ limit of the dot-dashed curve in Figs 3(a) and 6(a), with those using the saddle-point formula (30). For the latter we use b_0/b_{SP} obtained as the solution of (28) with $g_{NP} = 0.5$ GeV², and consider the two cases for the parton distributions participating in (30): “SP-I” uses the parton distributions which are obtained by evolving the customary NLO distributions at the scale Q , to b_0/b_{SP} using the NLO evolution operators up to the NNLL corrections like (13); “SP-II” uses the customary NLO distributions at the scale b_0/b_{SP} . Here the “customary NLO distributions” are constructed as described above (22). First of all, the results for SP-I demonstrate the remarkable accuracy of our simple analytic formula (30) for both RHIC and J-PARC, reproducing the results of NB to the 10% accuracy. ** On the other hand, the results for SP-II indicate that the NNLL corrections are moderate for large \sqrt{S} at RHIC, while those are expected to be small for small \sqrt{S} at J-PARC.

We propose that our simple formula (30) is applicable to the analysis of low-energy experiment at J-PARC in order to extract the NLO transversity distributions directly from the data. On the other hand, (30) will not be so accurate for analyzing the data at RHIC, but will be still useful for obtaining the first estimate of the transversities. We emphasize that such (moderate) uncertainty in applying our formula (30) to the RHIC case is not caused by the saddle-point evaluation, nor by considering the $Q_T \rightarrow 0$ limit, but rather is

^{||}This fact also suggests that one may use the fixed value, $b_0/b_{SP} \simeq 1$ GeV, in (30) for all Q (and g_{NP}) rather than solving (28) numerically for each different input value of Q , g_{NP} , because the sensitivity of the LO evolution on the small change of the scale is modest.

**If we use the fixed value, $b_0/b_{SP} = 1$ GeV, for all cases, instead of the solution of (28), the results in SP-I change by at most 5%, for both RHIC and J-PARC kinematics. The corresponding change in SP-II is by less than 5% for J-PARC, and by about 10% (15%) for $Q = 2\text{-}8$ GeV ($Q = 15\text{-}20$ GeV) at RHIC.

	$\sqrt{S} = 200 \text{ GeV}, \ y = 2$					$\sqrt{S} = 10 \text{ GeV}, \ y = 0$		
Q	2GeV	5GeV	8GeV	15GeV	20GeV	2GeV	2.5GeV	3.5GeV
SP-I	4.3%	5.4%	6.6%	8.7%	9.8%	14.1%	14.5%	14.8%
SP-II	7.3%	8.7%	9.8%	11.8%	12.7%	14.7%	14.8%	14.2%
NB	3.8%	4.9%	6.1%	8.2%	9.4%	13.4%	14.0%	14.9%

Table 3: The $Q_T \rightarrow 0$ limit of $\mathcal{A}_{TT}^{\text{NLL}}(Q_T)$ of (23) for RHIC and J-PARC kinematics. SP-I and SP-II are the results of the saddle-point formula (30) for $g_{NP} = 0.5 \text{ GeV}^2$, using the evolution operators from Q to b_0/b_{SP} , to the NLL accuracy and to the customary NLO accuracy, respectively. NB is obtained from the dot-dashed curve in Figs 3(a) and 6(a).

inherent in the general Q_T resummation framework which, at the NLL level, implies the use of the evolution operators (13) with the LO DGLAP kernel; more accurate treatment of the small- x region of the parton distributions relevant to the RHIC case would require the resummation formula to the NNLL accuracy, where the NLO DGLAP kernel participates in the evolution operators (13) from Q to b_0/b (see e.g. [14]).

5 Conclusions

In this paper we have presented a study of double transverse-spin asymmetries for dilepton production at small Q_T in pp collisions. The logarithmically enhanced contributions, which arise in the small Q_T region due to multiple soft gluon emission in QCD, are resummed to all orders in α_s up to the NLL accuracy. Based on this framework, we calculate numerically the spin-dependent and spin-averaged cross sections in tDY, and the corresponding asymmetries $\mathcal{A}_{TT}(Q_T)$, as a function of Q_T at RHIC kinematics as well as at J-PARC kinematics. The soft gluon resummation contributions make the cross sections finite and well-behaved over all regions of Q_T , so that the singular Q_T spectra in the fixed-order perturbation theory are redistributed, forming a well-developed peak in the small Q_T region. As a result, both the polarized and unpolarized cross sections become more “observable” around the pronounced “peak region” at small Q_T , involving the bulk of events. Reflecting the universal nature of the soft gluon effects, those large resummation-contributions mostly cancel in the cross section asymmetries $\mathcal{A}_{TT}(Q_T)$, leading to the almost constant behavior of $\mathcal{A}_{TT}(Q_T)$ in the small Q_T region, but, remarkably, the effects surviving the cancellation raise the corresponding constant value of $\mathcal{A}_{TT}(Q_T)$ considerably compared with the asymmetries in the fixed-order perturbation theory. We have obtained a QCD prediction as $\mathcal{A}_{TT}(Q_T) \simeq 5\text{-}10\%$ and 15-20% in the “flat region” for typical kinematics at RHIC and J-PARC, respectively, where the different values of $\mathcal{A}_{TT}(Q_T)$ are associated with the different values of parton’s momentum fraction probed by these two experiments.

We have also derived a new saddle-point formula for $\mathcal{A}_{TT}(Q_T \approx 0)$, clarifying the classification of the contributions involved in the resummation formula for $Q_T \rightarrow 0$. The formula is exact to the NLL accuracy, and embodies the above remarkable features of

soft gluon resummation effects at small Q_T in a compact analytic form. Our saddle-point formula may be compared with the data of $\mathcal{A}_{TT}(Q_T)$ in the peak region of the DY Q_T -spectrum, and thus provides us with a new direct approach to extract the transversity distributions from experimental data.

We mention that there is another kind of logarithmically enhanced soft-gluon contributions, subject to the so-called “threshold resummation”, besides those treated by the Q_T resummation. It is known that the threshold resummation effects on the cross sections can be important when the probed momentum fractions of partons are rather large like at J-PARC. The corresponding effects for tDY are studied [28] in $p\bar{p}$ collisions at GSI kinematics, and the results indicate that the threshold resummation effects will not be so significant for the kinematical regions corresponding to experiments at J-PARC, and, furthermore, will cancel mostly in the asymmetries.

We have revealed that the “amplification” of the double transverse-spin asymmetries $\mathcal{A}_{TT}(Q_T)$ at small Q_T is driven by the partonic mechanism participating at the NLL level, as the interplay between the large logarithmic gluon effects resummed into the universal Sudakov factor and the DGLAP evolutions specific for each channel. Thus similar phenomenon is anticipated also in $p\bar{p}$ collisions at the future experiments at GSI [29], where the large values are predicted for the Q_T independent asymmetry A_{TT} [28, 30]. The application of our Q_T resummation formalism to $p\bar{p}$ collision will be presented elsewhere [31].

Acknowledgments

We thank Werner Vogelsang, Hiroshi Yokoya and Stefano Catani for useful discussions and comments. The work of J.K. and K.T. was supported by the Grant-in-Aid for Scientific Research Nos. C-16540255 and C-16540266.

Appendix: Resummed cross section for unpolarized DY

In this appendix, we summarize the corresponding results for the unpolarized Drell-Yan process which are necessary to calculate the asymmetry $\mathcal{A}_{TT}(Q_T)$. Although all of them have already appeared in the literatures [18, 15], we will list them for the convenience of the reader.

The NLL resummed component, corresponding to (4) for the polarized case, reads,

$$\begin{aligned}
X^{\text{NLL}}(Q_T^2, Q^2, y) = & \int_0^\infty db \frac{b}{2} J_0(bq_T) e^{S(b, Q)} \left[H(x_1^0, x_2^0; b_0^2/b^2) \right. \\
& + \frac{\alpha_s(b_0^2/b^2)}{2\pi} \left\{ \int_{x_1^0}^1 \frac{dz}{z} C_{qq}^{(1)}(z) H(x_1^0/z, x_2^0; b_0^2/b^2) + \int_{x_2^0}^1 \frac{dz}{z} C_{qq}^{(1)}(z) H(x_1^0, x_2^0/z; b_0^2/b^2) \right. \\
& \left. \left. + \int_{x_1^0}^1 \frac{dz}{z} C_{qg}^{(1)}(z) K_2(x_1^0/z, x_2^0; b_0^2/b^2) + \int_{x_2^0}^1 \frac{dz}{z} C_{qg}^{(1)}(z) K_1(x_1^0, x_2^0/z; b_0^2/b^2) \right\} \right], \quad (31)
\end{aligned}$$

where $S(b, Q)$ is the exponent of the Sudakov factor, given by (5)-(11), and

$$\begin{aligned} C_{qq}^{(1)}(z) &= C_{\bar{q}\bar{q}}^{(1)}(z) = C_F (1 - z) + C_F \left(\frac{\pi^2}{2} - 4 \right) \delta(1 - z) , \\ C_{qg}^{(1)}(z) &= C_{\bar{q}g}^{(1)}(z) = 2 T_R z (1 - z) , \end{aligned}$$

with $T_R = 1/2$. The parton distributions are defined as,

$$\begin{aligned} H(x_1, x_2; \mu_F^2) &= \sum_q e_q^2 [q(x_1, \mu_F^2) \bar{q}(x_2, \mu_F^2) + \bar{q}(x_1, \mu_F^2) q(x_2, \mu_F^2)] , \\ K_1(x_1, x_2; \mu_F^2) &= \sum_q e_q^2 [q(x_1, \mu_F^2) + \bar{q}(x_1, \mu_F^2)] g(x_2, \mu_F^2) , \\ K_2(x_1, x_2; \mu_F^2) &= \sum_q e_q^2 g(x_1, \mu_F^2) [q(x_2, \mu_F^2) + \bar{q}(x_2, \mu_F^2)] . \end{aligned}$$

The finite component, corresponding to $\Delta_T Y$ of (3) for the polarized case, is given by,

$$Y(Q_T^2, Q^2, y) = \frac{\alpha_s(\mu_R^2)}{2\pi} [C_F Y_q(Q_T^2, Q^2, y) + T_R Y_g(Q_T^2, Q^2, y)] ,$$

where the first term comes from the $q\bar{q}$ annihilation subprocess as

$$\begin{aligned} Y_q(Q_T^2, Q^2, y) &= -\frac{2}{S} \left[\int_{\sqrt{\tau_+} e^y}^1 \frac{dx_1}{x_1 - x_1^+} \frac{H(x_1, x_2^*; \mu_F^2)}{x_1 x_2^*} + \int_{\sqrt{\tau_+} e^{-y}}^1 \frac{dx_2}{x_2 - x_2^+} \frac{H(x_1^*, x_2; \mu_F^2)}{x_1^* x_2} \right] \\ &+ \frac{1}{Q_T^2} \left[\int dx_1 H_1 + \int dx_2 H_2 + 2 H(x_1^0, x_2^0; \mu_F^2) \ln \frac{(1 - x_1^+)(1 - x_2^+)}{(1 - x_1^0)(1 - x_2^0)} \right] , \end{aligned}$$

with the variables according to [18, 6]:^{††}

$$\begin{aligned} x_1^+ &= \left(\frac{Q^2 + Q_T^2}{S} \right)^{1/2} e^y , \quad x_2^+ = \left(\frac{Q^2 + Q_T^2}{S} \right)^{1/2} e^{-y} , \\ x_1^* &= \frac{x_2 x_1^+ - x_1^0 x_2^0}{x_2 - x_2^+} , \quad x_2^* = \frac{x_1 x_2^+ - x_1^0 x_2^0}{x_1 - x_1^+} , \quad \sqrt{\tau_+} = \sqrt{\frac{Q_T^2}{S}} + \sqrt{\tau + \frac{Q_T^2}{S}} . \end{aligned}$$

We used the shorthand notation for the integral that vanishes for $Q_T = 0$,

$$\begin{aligned} \int dx_1 H_1 &\equiv \int_{\sqrt{\tau_+} e^y}^1 \frac{dx_1}{x_1 - x_1^+} \left[H(x_1, x_2^*; \mu_F^2) \left\{ 1 + \left(\frac{\tau}{x_1 x_2^*} \right)^2 \right\} - 2 H(x_1^0, x_2^0; \mu_F^2) \right] \\ &\quad - \int_{x_1^0}^1 \frac{dx_1}{x_1 - x_1^0} \left[H(x_1, x_2^0; \mu_F^2) \left\{ 1 + \left(\frac{x_1^0}{x_1} \right)^2 \right\} - 2 H(x_1^0, x_2^0; \mu_F^2) \right] , \end{aligned}$$

^{††}Note that $x_{1,2}^+ = \sqrt{\tau_+} e^{\pm y} = x_{1,2}^* = x_{1,2}^0$ when $Q_T^2 = 0$.

and $\int dx_2 H_2 = \int dx_1 H_1|_{y \rightarrow -y}$. For the contribution from the gluon Compton process, we have

$$\begin{aligned}
Y_g(Q_T^2, Q^2, y) = & \frac{1}{S} \left[\int_{\sqrt{\tau_+} e^y}^1 \frac{dx_1}{x_1 - x_1^+} K_1(x_1, x_2^*; \mu_F^2) \frac{x_1 x_2^+ - \tau}{(x_1 x_2^*)^2} \right. \\
& + \int_{\sqrt{\tau_+} e^{-y}}^1 \frac{dx_2}{x_2 - x_2^+} K_1(x_1^*, x_2; \mu_F^2) \frac{x_1^* x_2^+ - \tau}{(x_1^* x_2)^2} \left. \right] \\
& + \frac{1}{Q_T^2} \left[\int_{\sqrt{\tau_+} e^{-y}}^1 \frac{dx_2}{x_2 - x_2^+} K_1(x_1^*, x_2; \mu_F^2) \left\{ \frac{x_2 x_1^+ - \tau}{x_1^* x_2} - \frac{2\tau (x_2 x_1^+ - \tau)^2}{(x_1^* x_2)^3} \right\} \right. \\
& \quad - \int_{x_2^0}^1 \frac{dx_2}{x_2} K_1(x_1^0, x_2; \mu_F^2) \left\{ 1 - \frac{2x_2^0 (x_2 - x_2^0)}{x_2^2} \right\} \\
& \quad + \int_{\sqrt{\tau_+} e^y}^1 \frac{dx_1}{x_1 - x_1^+} K_1(x_1, x_2^*; \mu_F^2) \left\{ \frac{x_2^* x_1^+ - \tau}{x_1 x_2^*} - \frac{2\tau (x_2^* x_1^+ - \tau)^2}{(x_1 x_2^*)^3} \right\} \left. \right] \\
& + (1 \leftrightarrow 2) ,
\end{aligned}$$

where $1 \leftrightarrow 2$ means the exchange of the suffix of variables as well as $y \leftrightarrow -y$. As for the parton distributions, this exchange should be read,

$$K_1(x_1, x_2^*) \leftrightarrow K_2(x_1^*, x_2) , \quad K_1(x_1^*, x_2) \leftrightarrow K_2(x_1, x_2^*) , \quad K_1(x_1^0, x_2) \leftrightarrow K_2(x_1, x_2^0) .$$

The fixed-order cross section in the $\overline{\text{MS}}$ scheme is given as

$$\frac{d\sigma^{\text{FO}}}{dQ^2 dQ_T^2 dy d\phi} = \frac{2\alpha^2}{3 N_c S Q^2} [X(Q_T^2, Q^2, y) + Y(Q_T^2, Q^2, y)] , \quad (32)$$

to the $\mathcal{O}(\alpha_s)$ accuracy, where $X(Q_T^2, Q^2, y) \equiv X^{\text{NLL}}(Q_T^2, Q^2, y)|_{\text{FO}}$ denotes the “singular” part resulting from the expansion of the resummed component up to the fixed-order $\alpha_s(\mu_R^2)$. The formula (32) should be compared with (3). Taking the similar steps as those in (12)-(17), we obtain the differential cross section for unpolarized DY with the soft gluon resummation as

$$\frac{d\sigma}{dQ^2 dQ_T^2 dy d\phi} = \frac{2\alpha^2}{3 N_c S Q^2} \left[\tilde{X}^{\text{NLL}}(Q_T^2, Q^2, y) + \tilde{Y}(Q_T^2, Q^2, y) \right] , \quad (33)$$

which is used to calculate (20).

References

- [1] See e.g., V. Barone, A. Drago and P. G. Ratcliffe, Phys. Rep. **359**, (2002) 1; J. Kodaira and K. Tanaka, Prog. Theor. Phys. **101** (1999) 191.
- [2] M. Anselmino, et al., Phys. Rev. **D75** (2007) 054032.

- [3] J. P. Ralston and D. E. Soper, Nucl. Phys. **B152** (1979) 109; R. L. Jaffe and X. D. Ji, Nucl. Phys. **B375** (1992) 527.
- [4] O. Martin, A. Schäfer, M. Stratmann and W. Vogelsang, Phys. Rev. **D57** (1998) 3084; *ibid.* **D60** (1999) 117502.
- [5] A. Mukherjee, M. Stratmann and W. Vogelsang, Phys. Rev. **D67** (2003) 114006; A. Mukherjee, M. Stratmann and W. Vogelsang, Phys. Rev. **D72** (2005) 034011.
- [6] H. Kawamura, J. Kodaira, H. Shimizu and K. Tanaka, Prog. Theor. Phys. **115** (2006) 667.
- [7] D. Dutta et al., Letter of Intent (L15) for Nuclear and Particle Physics Experiments at J-PARC, <http://www-ps.kek.jp/jhf-np/LOIlist/LOIlist.html>.
- [8] Y. Koike, J. Nagashima and W. Vogelsang, Nucl. Phys. **B744** (2006) 59.
- [9] M. Contalbrigo, A. Drago and P. Lenisa, hep-ph/0607143, in Proceedings of XIV International Workshop on Deep Inelastic Scattering (DIS2006), Tsukuba, Japan, eds. M. Kuze et al. (World Scientific, 2007), p.727.
- [10] C. T. H. Davies and W. J. Stirling, Nucl. Phys. **B244** (1984) 337.
- [11] J. Kodaira and L. Trentadue, Phys. Lett. **B112** (1982) 66 ; Report **SLAC-Pub-2934** (1982); Phys. Lett. **B123** (1983) 335.
- [12] D. de Florian and M. Grazzini, Phys. Rev. Lett. **85** (2000) 4678.
- [13] E. Laenen, G. Sterman and W. Vogelsang, Phys. Rev. **D63** (2001) 114018; S. Kulesza, G. Sterman and W. Vogelsang, Phys. Rev. **D66** (2002) 014011.
- [14] S. Catani, D. de Florian and M. Grazzini, Nucl. Phys. **B596** (2001) 299; G. Bozzi, S. Catani, D. de Florian and M. Grazzini, Phys. Lett. **B564** (2003) 65; Nucl. Phys. **B737** (2006) 73.
- [15] J. C. Collins, D. Soper and G. Sterman, Nucl. Phys. **B250** (1985) 199.
- [16] X. Artru and M. Mekhfi, Z. Phys. **C45** (1990) 669.
- [17] A. Hayashigaki, Y. Kanazawa and Y. Koike, Phys. Rev. **D56** (1997) 7350; S. Kumano and M. Miyama, Phys. Rev. **D56** (1997) 2504; W. Vogelsang, Phys. Rev. **D57** (1998) 1886.
- [18] G. Altarelli, R. K. Ellis, M. Greco and G. Martinelli, Nucl. Phys. **B246** (1984) 12.
- [19] J. Soffer, Phys. Rev. Lett. **74** (1995) 1292.
- [20] M. Glück, E. Reya and A. Vogt, Eur. Phys. J. **C5** (1998) 461.

- [21] M. Glück, E. Reya, M. Stratmann, and W. Vogelsang, Phys. Rev. **D63** (2001) 094005.
- [22] A. Kulesza and W. J. Stirling, JHEP **0312** (2003) 056.
- [23] M. Gluck, E. Reya and A. Vogt, Z. Phys. **C67** (1995) 433.
- [24] M. Gluck, E. Reya, M. Stratmann and W. Vogelsang, Phys. Rev. **D53** (1996) 4775.
- [25] G. Parisi and R. Petronzio, Nucl. Phys. **B154** (1979) 427; J. C. Collins and D. E. Soper, Nucl. Phys. **B197** (1982) 446.
- [26] A. Kulesza and W. J. Stirling, Nucl. Phys. **B555** (1999) 279.
- [27] J. Qiu and X. Zhang, Phys. Rev. Lett. **86** (2001) 2724.
- [28] H. Shimizu, G. Sterman, W. Vogelsang and H. Yokoya, Phys. Rev. **D71** (2005) 114007.
- [29] V. Barone, et al.[PAX Collaboration], hep-ex/0505054; M. Maggiora et al. [ASSIA Collaboration], hep-ex/0504011.
- [30] V. Barone, A. Caferella, C .Coriano, M. Guzzi and P. G. Ratcliffe, Phys. Lett **B639** (2006) 483.
- [31] H. Kawamura, J. Kodaira and K. Tanaka, in preparation.